ВІСНИК ЛЬВІВ. УН-ТУ
Серія фіз. 2009. Вип. 43. С. 209–225

VISNYK LVIV UNIV.
Ser. Physics. 2009. Is. 43. P. 209–225

PACS number(s): 64.70.ph, 61.43 Fs, 81.05.Gc

STRUCTURAL MODELS OF LONG- AND SHORT-TERM PHYSICAL AGEING IN SELENIUM-RICH GLASSES

R. Golovchak

Lviv Scientific Research Institute of Materials of SRC "Carat"
202 Stryjska Str., UA-79031 Lviv, UKRAINE
e-mail: golovchak@novas.lviv.ua

Long-term and short-term physical ageing effects are studied in a Se-based chalcogenide glasses. The As-Se glasses having long Se_n chains ($n \geq 3$) in their structure as well as the glasses which network approaches a self-organized phase (optimally constrained network) are examined at the example of $As_{10}Se_{90}$ and $As_{30}Se_{70}$ compositions. Physical ageing processes are studied by combining the results of differential scanning calorimetry (DSC), X-ray photoelectron spectroscopy (XPS), extended X-ray absorption fine-structure spectroscopy (EXAFS), solid state ^{77}Se nuclear magnetic resonance (NMR) and Raman spectroscopy. Atomistic model of physical ageing is constructed using these data. Straightening-shrinkage processes of Se chain fragments are considered as the main microstructural mechanism of short-term physical ageing in Se-rich network glasses, while long-term physical ageing in underconstrained glasses with short chalcogen chains ($1 \leq n < 3$) is attributed to cooperative many-body relaxation dynamics, slowed down by the rigidity of short polymeric Se-chains below glass transition temperature.

Key words: physical ageing, chalcogenide glasses, EXAFS, NMR, DSC, Raman spectroscopy.

Chalcogenide glasses (ChG) are known for long years as perspective solid state media for potential applications in optoelectronics [1–3]. Nevertheless, their atomic structure and, consequently, physical properties change with time essentially restricting their practical implementation [3–8]. The reason is that ChG are conventionally obtained in a metastable state frozen near glass transition and therefore they aspire with time to the extrapolated states of thermodynamic equilibrium of undercooled liquid. This effect occurred under normal conditions is known as natural physical ageing [7, 8].

It was shown recently for As-Se and Ge-Se binary ChG that the most significant natural physical ageing occurs in Se-rich samples [7, 8]. So, it was assumed that nature of this effect was associated with the existence of -Se-Se-Se- segments in the network of such ChG glasses [7, 8]. The compositional dependence of physical ageing effect in very old glasses (~20 years) revealed also dependence of this effect on a length of Se polymeric chain. Therefore, short-term and long-term components of natural physical ageing were distinguished [7, 9]. However, the actual mechanisms of them and convenient explanation have not been developed.

In the present paper, a mechanism of physical ageing in Se-based network ChG is proposed on the basis of extended X-ray absorption fine-structure (EXAFS), solid state ^{77}Se nuclear magnetic resonance (NMR), differential scanning calorimetry (DSC) and Raman spectroscopy results. The $As_{10}Se_{90}$ composition is chosen as a model object for the investigations of microstructural processes in glass network with long polymeric chains, while the $As_{30}Se_{70}$ composition is typical representative of ChG with short chalcogen chains close to rigidity percolation point.

The vitreous $As_{10}Se_{90}$ and $As_{30}Se_{70}$ samples were prepared in 1985 by a standard melt quenching method using a mixture of high purity (99,999%) precursors sealed in evacuated quartz ampoules. Until the present experiment, the ingot was stored in hermetically sealed plastic bags, in the dark at room temperature. The amorphous state of ChG was established visually from a conch-like fracture and X-ray diffraction data. The composition was checked before the experiment by X-ray photoelectron spectroscopy (XPS). Parts of ~20 years aged ChG ingot were rejuvenated before EXAFS, NMR and Raman measurements, by heating up to the temperature 50 K above glass transition temperature (T_g) and then quenching to room temperature. This procedure was performed in microcalorimeter DSC 404/3/F (NETZSCH, Germany), which was also used to determine the physical ageing effect in the samples. The heating rate of q = 5 K/min, was used for revealing physical ageing effect by DSC, whereas for rejuvenation q = -5 K/min was used in the cooling mode. After this procedure, the samples were in the thermodynamic state close to the initial as-prepared condition.

To perform EXAFS measurements, 20-years aged and rejuvenated samples were powdered and stuck onto a 'Kapton' tape. EXAFS experiments were performed at X18B X-ray beamline at National Synchrotron Light Source, Brookhaven National Laboratory. The wavelength of the synchrotron X-ray was selected by a Si (111) channel cut monochromator with detuning and deglitching capabilities. A white beam slit of vertical height 1 mm and horizontal size 3 mm was used just up stream of the monochromator. Data collection was performed at the As K-edge (11,863 KeV) and Se K-edge (12,658 KeV) in transmission mode using sealed ion chambers of Oxford Danfysic filled with Ar/N_2 gases. The energy of the Se K-edge was calibrated using pure Se as standard.

The EXAFS signal presents modulation in the absorption coefficient (μ_i) as a function of X-ray energy ($E = \hbar\omega$). Using one-electron approximation of Fermi's Golden Rule for $\mu_i(\omega)$, under the plane wave approximation, the EXAFS equation for isotropic materials can be expressed as [10]:

$$\mu_i(k) = \frac{\mu_1(k)}{\mu_0(k)} = \sum_j \frac{N_j F_j(k) S_0^2(k) \cdot \sin(2kR_j + \phi_j(k))}{kR_j^2 \cdot \exp\left(\frac{2R_j}{\Lambda} + 2k^2\sigma_j^2\right)}, \quad (1)$$

where $\mu_1(k)$ and $\mu_0(k)$ are the terms contributed by the background and single scattering, respectively (multiple scattering terms are negligible for EXAFS region); $k \approx 0{,}512(E\text{-}E_0)^{1/2}$ Å^{-1} is the wavevector of photoelectron, E_0 – the threshold energy; N_j – number of neighbours in the jth shell at an average distance R_j; $F_j(k)$ is the amplitude of backscattered electron wave, $\phi_j(k)$ – phase shift between backscattered and outgoing electron wave; S_0 is an amplitude reduction factor caused by many-body relaxation effects; Λ is the mean free path of photoelectrons and σ_j – the Debye-Waller factor related with disorder.

Standard Athena-Artemis software package was used to process experimental EXAFS spectra [11]. The information on $F_j(k)$ and $\phi_j(k)$ was obtained using crystallographic data of As_2Se_3 crystal [12] and trigonal selenium [13] as input. Kaiser-Bessel type of window function was used for restricting the EXAFS data in k space.

The Raman spectra were obtained by using a Fourier Transformation IFS 55 spectrophotometer with FRA 106 accessory (Bruker, Germany). The pumping beam of Nd:YAG laser (λ = 1,064 μm) with the output power 90 mW was used for the excitation of the Raman spectra. The resolution of the Raman spectrometer was 1 cm^{-1} at 100 scans.

The ^{77}Se (I = 1/2) NMR experiments were carried out at room temperature on an ASX 300 Bruker spectrometer operating at 57,3 MHz with a 2,5 mm Magic Angle Spinning probe rotating at 22 kHz. Due to the breadth of the NMR lines for glasses, a Hahn spin echo sequence was applied to refocus the whole magnetization. The Fourier transforms were performed on the whole echoes to increase the signal-to-noise ratio and to directly obtain some absorption mode line shapes. Because of the slow longitudinal relaxation processes, the recycle time was equal to 30 s. Owing to the weak sensitivity the numbers of scans were between 2 000 and 10 000. The simulations of the experimental spectra were performed using the Dm2000nt version of the Winfit software [14]. The external reference used for the chemical shifts is Me_2Se in deuterated chloroform [15].

DSC data for two $As_{10}Se_{90}$ ChG samples after ~20-years of natural storage, and just after rejuvenation are shown in fig. 1. The huge increase in T_g (about 30 K) and endothermic peak area (~10 times) in the vicinity of glass-to-undercooled liquid transition testifies the significant natural physical ageing effect in this ChG [7]. It should be noted here that the endothermic peak area is directly proportional to the enthalpy losses occurred during prolonged natural storage of the samples. The DSC data for $As_{30}Se_{70}$ ChG after ~20-years of natural storage demonstrates significant natural physical ageing in this specimen too [7, 9].

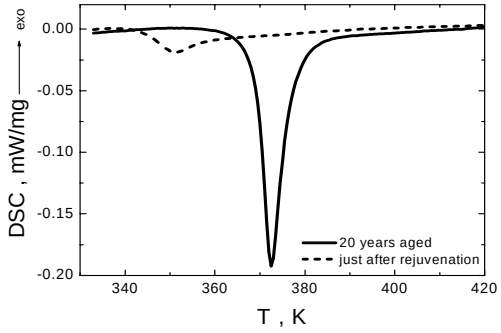

Fig. 1. DSC traces of 20-years old and rejuvenated vitreous $As_{10}Se_{90}$ samples

It was previously shown that the observed long-term physical ageing effect was not a consequence of difference between DSC heating and melt-quenching rates and/or thermal annealing at near-T_g temperatures after synthesis [9]. The kinetics of long-term natural physical ageing for rejuvenated (q^- = 5 K/min) ChG sample (fig. 2) showing the decrease in fictive temperature (T_F) determined by equal square method [16], obeys

exponential law kinetics $\exp\left(-\frac{t}{\tau}\right)$ with characteristic relaxation time $\tau \approx 20$ years. This magnitude is typical for long-term physical ageing (tens of years) at room temperature, as observed previously in various silicate glasses [17, 18].

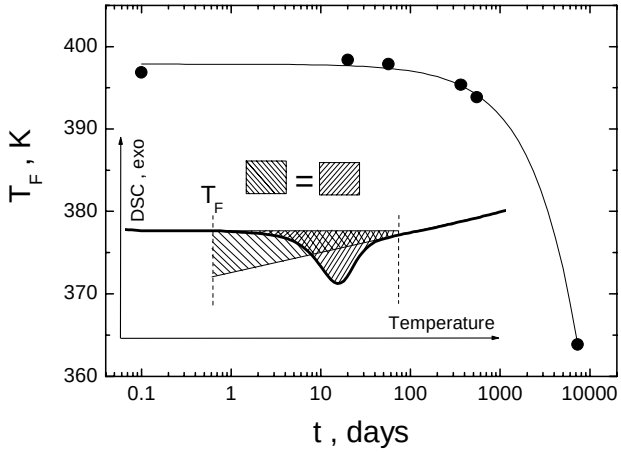

Fig. 2. Evolution of fictive temperature T_F during natural storage (the solid line represents the fit, insert shows the equal square method for T_F calculation [16])

Since short-term component of natural physical ageing effect was assumed to be connected with the existence in glass structure of elementary -Se-Se-Se- segments [7, 8], let us consider only the inner Se atoms within a Se_n chain (for present discussion, we consider Se_n chain as a linear sequence of n Se atoms between two As atoms). It is well known that these atoms form soft, flexible configurations, characterized by a so-called double-well potential with ~kT energetic barrier (fig. 3) [19–21].

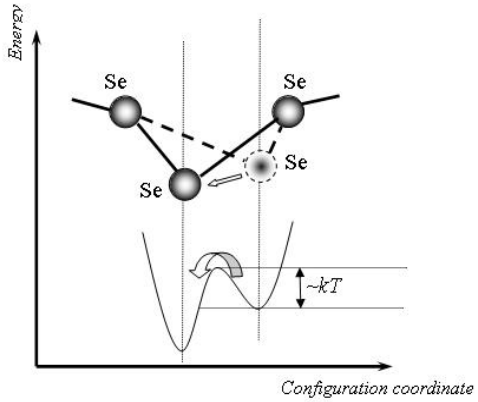

Fig. 3. Boundary displacement of bridge chalcogen atom along -Se-Se-Se- cell towards a more equilibrium thermodynamic state within local double-well potential

It means that the inner Se atoms can occupy two different states within their polymeric chains (say *cis* and *trans* configurations) without significant energy perturbations. This feature is appropriate only for the inner (i.e. not at the two ends) atoms of Se_n chains and does not occur in bulk ChG when $n < 3$. Since by definition glass is a system not in thermodynamic equilibrium after synthesis (rejuvenation or in as-prepared state) [6], a significant number of Se atoms may not occupy the most energetically favourable positions within the glass structure. Then their transition into more energetically favourable states (shown by arrow in fig. 3) can serve as an elementary low-energy act of physical ageing. These elementary relaxation acts started in different places of the sample attain a cooperative nature by initiating the similar processes within parent and/or neighbouring Se chains (depending on their steric constraints, of course) due to inter- and intra-chain interactions. It is reasonable to suppose that such cooperative process is associated with the straightening of Se-based structural fragments and their better space utilization (fig. 4), because straightened/aligned Se chains occupy less geometrical volume than the bent ring-like configurations (in this sense, they can be considered as energetically more favourable). This assumption is supported by the molecular dynamics simulations in amorphous selenium showing that Se chains, which contain ring-like fragments (Se atoms in *cis* configuration), are energetically unstable and tend to be excluded from the samples [22]. The straightened fragments (Se atoms in *trans* configuration) cause decrease in the total ChG volume (and, consequently, the corresponding increase in glass density and T_g) because of shrinkage effect (fig. 4) similar to the experiments [23] and prevalent explanation [24] of ageing phenomenon in porous ceramics. In spite of their complex nature, these straightening-shrinkage structural transformations should manifest in all Se-rich compositions of As(Ge)-Se ChG containing $Se_{n \geq 3}$ chains. They are fast enough to cause conventional short-term physical ageing in these glasses. It is easy to show within the chains-crossing model (recently validated for As-Se ChG by solid-state nuclear magnetic resonance technique [25]) that $As_{25}Se_{75}$ composition is the first composition with minimum As content, where -Se-Se-Se- chains would disappear completely. We believe that the low limit of the reversibility window (compositional range where non-reversible heat flow is equal to zero), observed by temperature-modulated DSC in As-Se system at $As_{28}Se_{72}$ composition [26], is directly connected with the disappearance of these fragments.

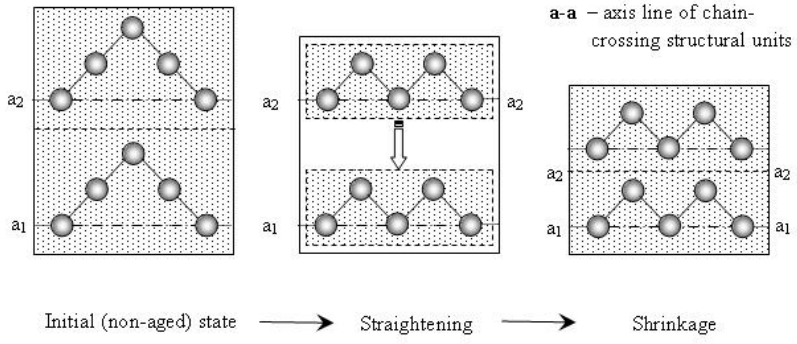

Fig. 4. Schematic illustration showing subsequent stages of straightening/alignment and shrinkage effects in Se-rich covalent-bonded glass backbone caused by short-term physical ageing (occupied volume is crosshatched)

It should be mentioned here that long-term physical ageing was also observed in As-Se ChG within the compositional range from $As_{25}Se_{75}$ to $As_{40}Se_{60}$ [7]. In principle, the ageing mechanism for these under-constrained ChG without Se-Se-Se fragments associated with network shrinkage may be qualitatively similar to that developed for silicate glasses [27]. However, much lower dissociation energies of chalcogenide bonds (within ~1,5–2,8 eV range) [28, 29] compared to that of the Si-O bond (~4,6 eV) [28] together with the possibility of chalcogen-chalcogen bond formation (in the case of silicate glasses O-O bonds do not exist) [28], introduce additional possibility for covalent bond switching accompanying physical ageing in ChG. However, the atomistic model for physical ageing in these ChG does not include relatively fast straightening-shrinkage processes described above (the short-term physical ageing was not detected in these ChG compositions [27]) because of a lack of $Se_{n\geq 3}$ chains. It is associated only with pure shrinkage of under-constrained glass network due to the excess of free volume frozen during quenching [7]. This process needs much longer duration of natural storage (decades of years) to be detected experimentally. It vanishes in $As_{40}Se_{60}$ ChG [7], in full agreement with rigidity percolation theory [30].

The shrinkage process during natural storage is already known from literature as time-dependent decrease of molar volume [23, 31], while the straightening process and bonds redistribution still need to be demonstrated. To confirm it experimentally, we use Raman spectroscopy, which allows observation of ring-like (bent-deformed chains or Se atoms in *cis* configurations) and chain-like (straightened chains or Se atoms in *trans* configurations) Se fragments [32–35], as well as changes in bonds statistics. The Raman spectra of 20-years aged and rejuvenated $As_{10}Se_{90}$ and $As_{30}Se_{70}$ ChG as well as their difference are presented in fig. 5. The observed band components (ξ) in fig. 5a for $As_{10}Se_{90}$ ChG have been assigned to $AsSe_3$ pyramidal units (~230 cm^{-1}), Se_n chains (240–250 cm^{-1}) and Se ring-like fragments (250–260 cm^{-1}) [22, 32–35]. The band of negative intensity ($\Delta\xi$) at ~260 cm^{-1} in the insert to figure 5, *a* directly corresponds to the disappearance of Se ring-like fragments (*cis* configurations of Se atoms in chain) as shown in fig. 4. The appearance of straightened/aligned Se_n chains instead of ring-like units can be associated with the band of positive intensity at ~250 cm^{-1} in the insert to figure 5, *a*. The observed peaks in the intensity (ξ) of band components in Raman spectra of aged and rejuvenated $As_{30}Se_{70}$ ChG (fig. 5, *b*) have been assigned to bond-stretching vibrations of directly corner-shared (~230 cm^{-1}) or Se-Se shared (~240 cm^{-1}) $AsSe_{3/2}$ pyramidal units and Se_3 segments (~250-260 cm^{-1}) [33–35]. The weak changes after prolonged natural storage are seen in the difference spectrum between aged and rejuvenated samples (see insert to fig. 5, *b*). The band of positive intensity change ($\Delta\xi$) at ~260 cm^{-1} is assigned to the appearance of Se-Se-Se fragments and one at ~230 cm^{-1} to the formation of As-Se-As fragments or corner shared $AsSe_{3/2}$ pyramids as a result of long-term physical ageing. Then, a decrease in the band intensity due to Se-Se shared $AsSe_{3/2}$ pyramids at ~240 cm^{-1} is expected, but not seen. We believe it is masked in the experimental Raman spectra by overlapping with peaks attributed to former two processes of opposite direction. Analysis of broad features in 80–150 cm^{-1} range corresponding to bond-bending vibrations is more complicated because of the overlap of different vibrational modes.

The slight increase of Se-Se-Se (~860 ppm), As-Se-As (~380 ppm) and decrease of Se-Se-As (~580 ppm) sites in the structure of aged $As_{30}Se_{70}$ ChG can be found by appropriate fitting of ^{77}Se NMR spectra (fig. 6, *b*) too, while NMR data for

$As_{10}Se_{90}$ ChG (fig. 6, *a*) show invariance of chains-crossing model during physical ageing for this specimen.

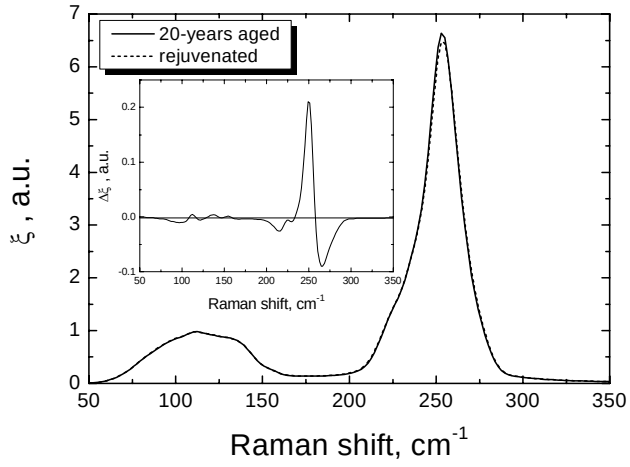

a

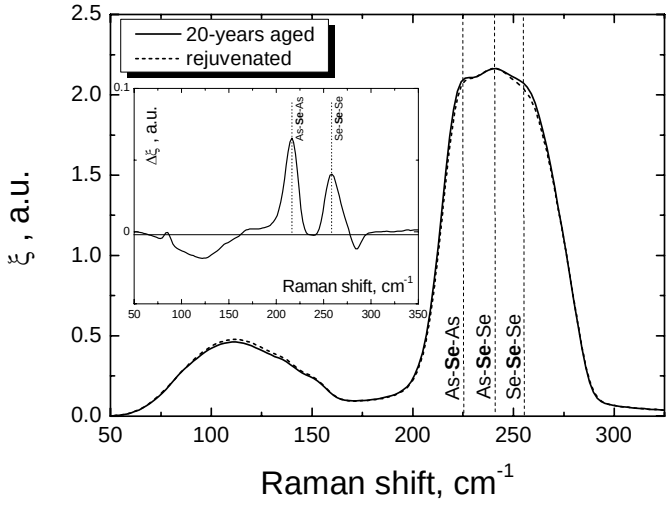

b

Fig. 5. Raman spectra of 20-years aged and rejuvenated vitreous $As_{10}Se_{90}$ (*a*) and $As_{30}Se_{70}$ (*b*) samples. Inserts show the difference between aged and rejuvenated curves

The lines are identified from NMR data obtained earlier for vitreous $As_{10}Se_{90}$, $As_{23}Se_{77}$ and $As_{40}Se_{60}$ (Fig. 6) rich in Se-Se-Se, Se-Se-As and As-Se-As structural fragments, respectively [25]. So, although the changes observed for $As_{30}Se_{70}$ ChG after 20-years of physical ageing are weak (in the case of NMR they only slightly exceed the

noise level), both Raman and NMR methods support the idea that two As-Se-Se-As structural units transform into As-Se-As and As-Se-Se-Se-As fragments during prolonged natural storage of vitreous $As_{30}Se_{70}$.

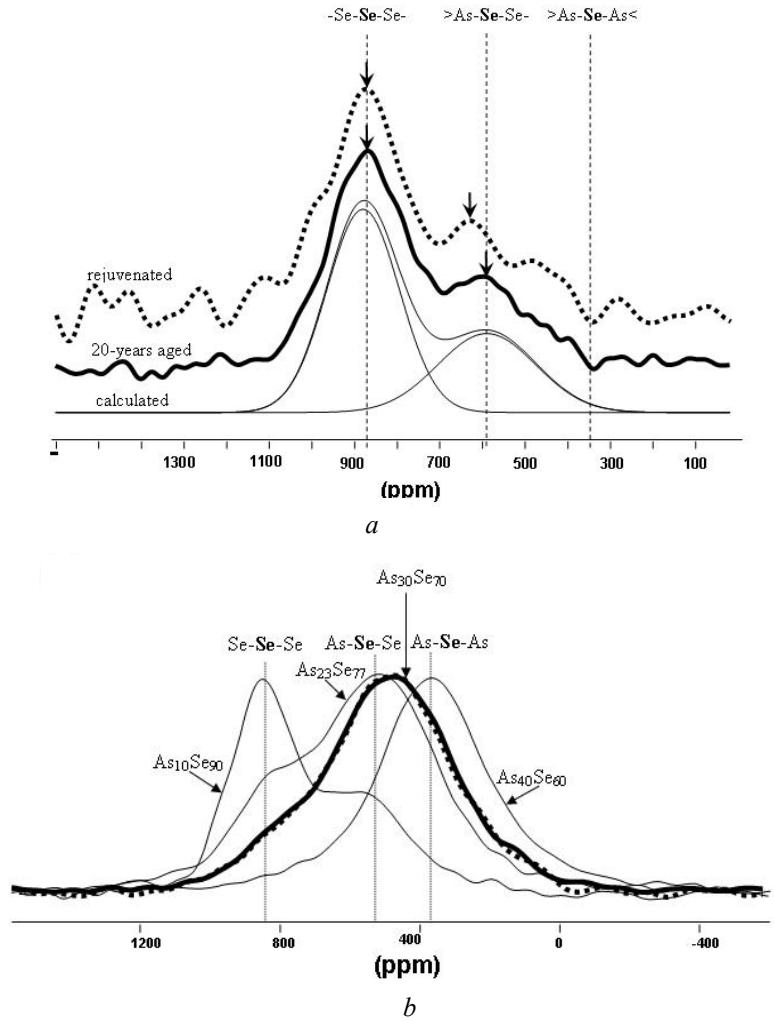

Fig. 6. Solid state Se^{77} NMR spectra of 20-years aged and rejuvenated vitreous $As_{10}Se_{90}$ (*a*) and $As_{30}Se_{70}$ (*b*)

The same conclusion is supported by high resolution XPS data for Se and As core levels of $As_{30}Se_{70}$ sample, which allow us to determine the relative fractions of the transformed complexes. Fitting parameters, such as peak position or binding energy (BE), partial area (*S*) and full width at half maximum (FWHM) are given in table 1. On the basis of electronegativity data [36] and compositional dependence of As-Se XPS

spectra [37], the Se 3*d* doublets with the intensity of primary components at ~54,8 eV were attributed to Se-Se-Se, at ~ 54,4 eV to As-Se-Se and at ~54,0 eV to As-Se-As structural fragments. The As core level was fitted by only one As 3*d* doublet with the intensity of main component at ~42,2 eV for both aged and rejuvenated samples (figure 5), which was assigned to Se-As<$(Se)_2$ regular environment. The results in table 1 show that the initial ratio of (Se-Se-Se) : (Se-Se-As) : (As-Se-As) structural fragments for rejuvenated samples is 3% : 69% : 28%, which is quite close to the values (S^0 in table 1) theoretically predicted by the "chains crossing model" for this composition: 0% : 72% : 28% [25]. After 20 years of natural storage this proportion deviates much more from this model, becoming 6% : 62% : 32% (table 1). Overall, we can conclude from these XPS results that long-term physical ageing leads to conformation of some Se-Se-As complexes into Se-Se-Se and As-Se-As structural fragments in good agreement with the results obtained by NMR and Raman spectroscopy.

Table 1

Binding energy (BE), full-width-at-half-maximum (FWHM) of the various structural units obtained from curve fitting of Se $3d_{5/2}$ and As $3d_{5/2}$ core level spectra. S^0 and S are the fraction of atomic units calculated theoretically using the "chains crossing model", and from experimental data, respectively

CORE LEVEL / SAMPLE	AS-SE-AS				SE-SE-AS			
	BE (EV)	FWHM (EV)	S (%)	S^0 (%)	BE (EV)	FWHM (EV)	S (%)	S^0 (%)
AGED	53,97	0,66	32	28	54,38	0,71	62	72
REJUVENATED	53,97	0,69	28	28	54,38	0,82	69	72

CORE LEVEL / SAMPLE	SE-SE-SE				SE-AS<$(SE)_2$			
	BE (EV)	FWHM (EV)	S (%)	S^0 (%)	BE (EV)	FWHM (EV)	S (%)	S^0 (%)
AGED	54,82	0,48	6	0	42,27	0,62	100	100
REJUVENATED	54,85	0,45	3	0	42,21	0,72	100	100

An indirect confirmation of straightening-shrinkage processes in vitreous $As_{10}Se_{90}$ can be obtained by EXAFS, because it is sensitive to changes in the local coordination number around target atom, to the distances in the coordination shells, as well as to the average deviations in bond lengths and angles (mean square relative displacement or the so-called Debye-Waller factor). The differences between 20-years aged and rejuvenated $As_{10}Se_{90}$ samples are seen in Fourier transformed (FT) EXAFS spectra in fig. 7 (the high quality of fits of EXAFS k^3-weighted oscillations $\chi(k)$ of both As and Se K-edges for the present samples is evident in the inserts to this figure). The well-pronounced peak in partial radial distribution functions associated with the first coordination shell and minor peaks at longer distances attributed to second and further coordination shells are typical of glassy materials [38, 39]. For the present work we have analyzed only the first coordination shell, which has much better signal-to-noise ratio. The fitting parameters

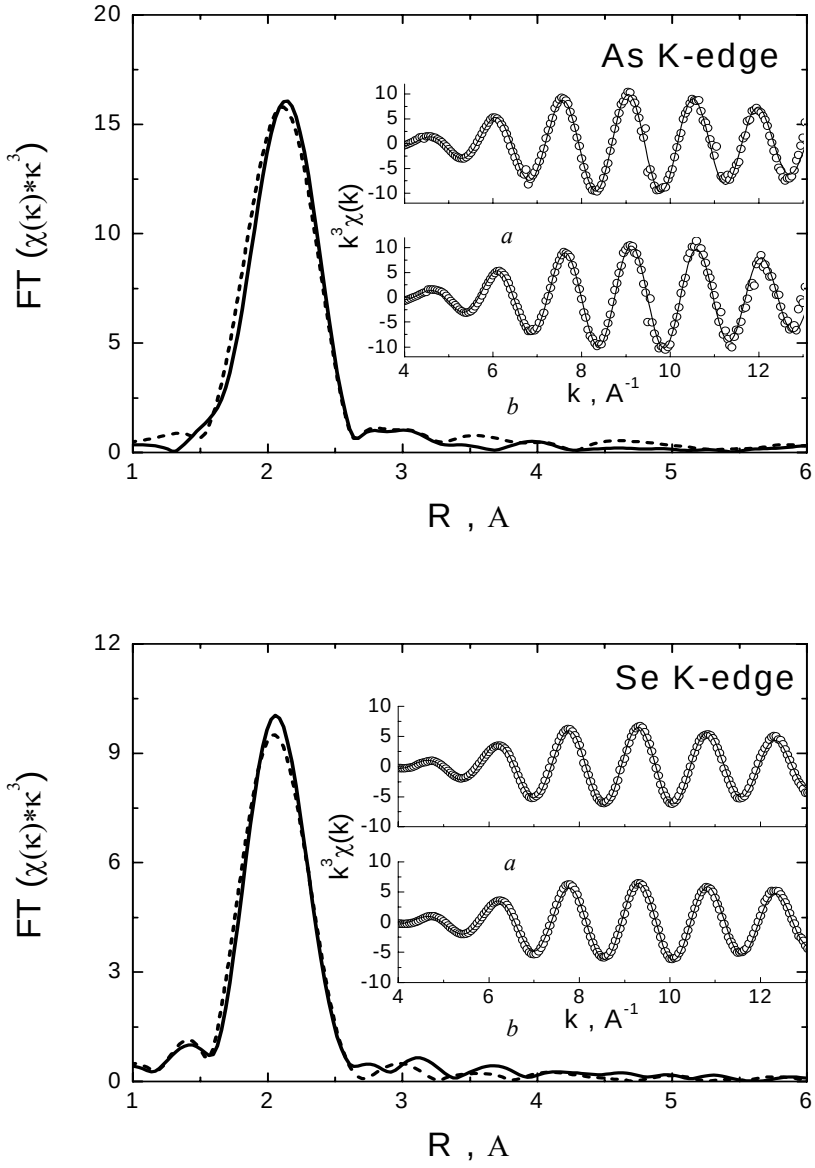

Fig. 7. Fourier transformed EXAFS spectra of $As_{10}Se_{90}$ glass taken at As and Se K-edges in rejuvenated (dash) and 20-years aged (solid) states. k^3-weighted EXAFS oscillations $\chi(k)$ (open circles) and their best fits (solid lines) according to data in table 2 are shown as inserts for (*a*) 20-years aged and (*b*) rejuvenated vitreous $As_{10}Se_{90}$

(table 2) show increase in the local coordination number N_j for Se K-edge, distance R_j for As K-edge and Debye-Waller factor σ^2 for both of them after 20 years of natural storage. Shrinkage process can directly result in the increase of N_{Se} because the distance between the atoms belonging to different Se_n chains decreases. When this distance becomes comparable with the length of covalent bond, the appropriate Se atoms contribute to an EXAFS signal in the *R*-range, associated, normally, with the nearest covalently-bonded atoms in the first coordination shell [38]. This could be the reason for increase in the disorder of average bond distances between nearest atoms, revealed through the increase in fitted Debye-Waller factor σ^2 for Se K-edge after 20-years of ageing (table 2).

Table 2

Fitting parameters for Se and As K-edge Fourier transformed EXAFS spectra of vitreous $As_{10}Se_{90}$: N_j – local coordination number; R – the distance from neighbouring atom to the absorbing atom; σ – the standard deviation of the interatomic distance; Re_{Chi} – reduced chi-square values for appropriate fitting

SE K-EDGE (12.658 KEV)				
DESCRIPTION	N_{SE}	R , Å	σ^2 , (Å ^{2})	RE_{CHI}
20 YEARS AGED	2,1±0,1	2,36±0,01	$(49\pm5)\cdot10^{-4}$	66
REJUVENATED	1,8±0,1	2,35±0,01	$(41\pm5)\cdot10^{-4}$	384
AS K-EDGE (11,863 KEV)				
DESCRIPTION	N_{AS}	R , Å	σ^2 , (Å ^{2})	RE_{CHI}
20 YEARS AGED	3,4±0,2	2,43±0,01	$(48\pm5)\cdot10^{-4}$	10
REJUVENATED	3,2±0,2	2,40±0,01	$(40\pm5)\cdot10^{-4}$	21

Since Se-Se bond distance in molecular ring clusters like Se_8 and Se_6 (the same should be valid also for ring-like fragments) is ~0,02–0,04 Å less than in Se_n polymeric chains [40], the straightening of ring-like fragments should result in its slight increase. There appears to be a tendency of this expected change in the first coordination peak for Se in Figure 7. It should be noted here that the experimental values of *R* are in excellent agreement with those obtained by X-ray diffraction measurements in this ChG [41]. Another support for chain straightening can be obtained by comparing the reduced chi-square (Re_{Chi}) values [42] for the fitting of the first coordination shell in Fourier transformed EXAFS spectra of Se K-edge (see table 2). For estimation of fitting parameters we used as input the crystallographic data of trigonal selenium [13], which consists of only Se chains. As far as Re_{Chi} value for 20-years aged samples is nearly 5 times smaller than for rejuvenated samples, it can be concluded that the structure of trigonal selenium more closely describes the structure of 20-years aged samples than that of the rejuvenated sample [42].

To understand the increase in *R* and σ^2 for As atoms, the straightening-shrinkage processes should be considered in a three-dimensional space. According to the chains-crossing model, the structure of $As_{10}Se_{90}$ ChG is represented as uniformly distributed $AsSe_3$ pyramids that cross-link Se_n chains. So, only -Se-Se-Se- and >As-Se-Se- fragments are expected in the environment of Se atoms in this glass. According to this model their ratio is theoretically predicted as 67% : 33% [25]. This ratio is close to the value experimentally determined from solid state NMR spectra (Fig. 6a) as the ratio between integrated intensities of corresponding lines at ~860 ppm (-Se-Se-Se- fragments) and at ~580 ppm (>As-Se-Se- fragments). Both the lines keep the same ratio

(65% : 35%) for rejuvenated and aged $As_{10}Se_{90}$ samples giving an evidence for the invariance of chains-crossing model during physical ageing. The line at ~380 ppm, which could be attributed to the >As-Se-As< complexes, is observed neither for 20-years aged nor for rejuvenated ChG, in agreement with the above model. Monte Carlo simulation of Se-rich ChG structure [43] allows one to schematically represent the cross-linked Se chains between $AsSe_3$ pyramids as spheres of ~15–20 Å diameter interlinked by As atoms (fig. 8). When straightening-shrinkage processes occur, they lead to the decrease in the volume of these virtual spheres. Taking place independently in each individual region, these processes cause general shrinkage of glass matrix (it is under-constrained in terms of Phillips and Thorpe [30]) and, as a result, deforming the As-Se bonds that interlink the Se-rich regions (fig. 8). This change leads to the observed increase of fitted As-Se distances and σ^2 values in the EXAFS spectra of 20-years aged $As_{10}Se_{90}$ ChG, as well as greater chemical shift (on ~ 30 ppm) of >As-Se-Se- line in the NMR spectra of rejuvenated samples (fig. 6**,** *a*).

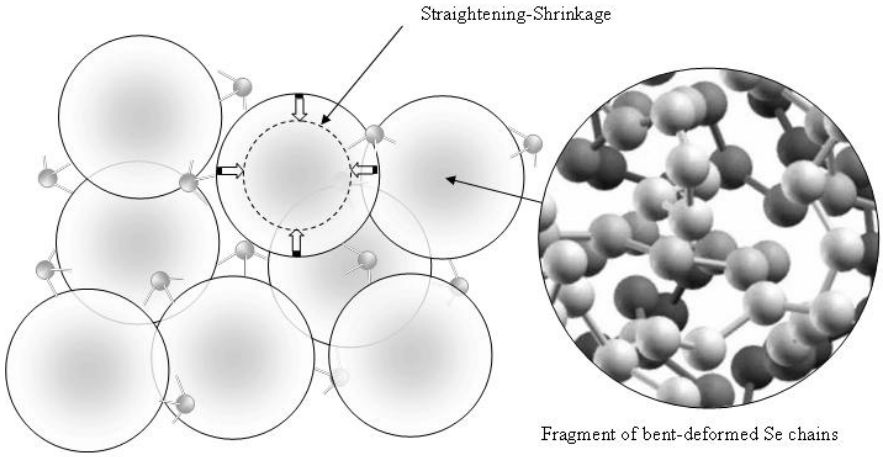

Fig. 8. Schematic representation of physical ageing in vitreous $As_{10}Se_{90}$ through straightening-shrinkage processes. Simulated structure of Se chains is taken from [43]

Table 3

Fitting parameters for Se and As K-edges Fourier transformed EXAFS spectra of vitreous $As_{30}Se_{70}$: N_j – local coordination number; R – the distance from neighbouring atom to the absorbing atom; σ – the standard deviation of the interatomic distance.

SE K-EDGE (12,658 KEV)			
DESCRIPTION	N_{SE}	R (Å)	σ^2 (Å^2)
20 YEARS AGED	2,0±0,1	2,38±0,01	0,0047±0,0003
REJUVENATED	2,3±0,2	2,39±0,01	0,0060±0,0004
AS K-EDGE (11,863 KEV)			
DESCRIPTION	N_{AS}	R (Å)	σ^2 (Å^2)
20 YEARS AGED	3,3±0,3	2,42±0,01	0,0045±0,0004
REJUVENATED	3,6±0,3	2,42±0,01	0,0053±0,0004

The fitting parameters of EXAFS spectra for $As_{30}Se_{70}$ samples (table 3) do not show any significant changes in average interatomic distances (R_j) or coordination number (N_j) after 20 years of natural storage for both As and Se elements. Thus, we do not find evidence for the formation of coordination defects or broken bonds in significant concentration. Taking into account Raman, NMR and XPS data for $As_{30}Se_{70}$ samples, we expect a microstructural mechanism of physical ageing for ChG with short chalcogen chains as follows. Let us consider four $AsSe_{3/2}$ pyramids coexisting in a manner shown in figure 9. Then, let us assume that I and II pyramidal units are in floppy and III and IV units are in rigid configurations. As an example of such situation, we can consider III and IV pyramids connected with their environment through direct corner-sharing (such configuration is optimally constrained [30], typical for stoichiometric $As_{40}Se_{60}$ ChG) and I and II pyramids connected with their environment by Se-Se sharing (thus, they are underconstrained). Let us consider a variant when pyramid I in a floppy configuration starts rotating (fig. 9) due to some relaxation processes. Since Se-Se (~1,91 eV) covalent bonds are stronger than As-Se (~1,77 eV) bonds [36], the As-Se bond of pyramid II becomes more distorted and finally breaks with greater probability than Se-Se bond, because the motion of pyramid II is restricted by the environment. The required energy for bond breaking can be accumulated from appropriate number of atoms or building blocks which participate in cooperative relaxation process, like in the case of silicate glasses [17,18]. After the As-Se bond of pyramid II is broken, the switching of Se-Se bond between pyramids III and IV takes place (fig. 9), most probably because of less distortions in the Se-Se bond length/angle within Se-Se-Se fragment in comparison to those caused by Se-Se sharing of pyramids in rigid configurations. Due to the volume collapse from general shrinkage of glass matrix (experimentally observed by S. Chakravarty et.al. [23] and C.T. Hatch et.al. [31]), the pyramids II and III become corner shared.

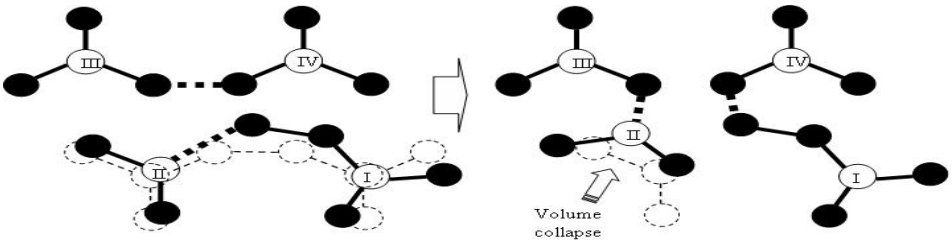

Fig. 9. Schematic presentation of bond-changing structural transformations in vitreous $As_{30}Se_{70}$ associated with long-term physical ageing (the switched bonds are highlighted; previous positions of structural complexes are shown by dash line)

Straightening-shrinkage processes of Se chain fragments are considered as the main microstructural mechanism of physical ageing in $As_{10}Se_{90}$ ChG as a typical representative of Se-rich network glasses. The straightening is proven by Raman spectroscopy through a decrease in the intensity of the band associated with ring-like fragments and an increase in the intensity of the band related to Se chains after prolonged natural storage samples. We suggest that the shrinkage processes, which also occur during physical ageing, are responsible for an increase in the local coordination number of the Se atoms, the Debye-Waller factors, and the As-Se distances determined from the Se and As K-edge EXAFS spectra, respectively. The increase in As-Se bond lengths after natural storage is also supported by solid-state Se^{77} NMR measurements

through a shift of the line attributed to >As-Se-Se- complexes. The NMR results show also that the chain-crossing model is invariant during physical ageing in ChG with long polymeric chains.

Long-term physical ageing in underconstrained vitreous $As_{30}Se_{70}$ (typical representative of ChG with short chalcogen chains) is attributed to cooperative many-body relaxation dynamics, slowed down by the rigidity of short polymeric Se-chains below T_g. The major driving force for physical ageing is volume contraction as in other polymeric materials. It arises from pure shrinkage of $As_{30}Se_{70}$ underconstrained glass network, as well as the re-conformation of some Se-Se shared $AsSe_{3/2}$ pyramids (As-Se-Se-As structural fragments) into directly corner-shared (via As-Se-As bridges) pyramids and Se-Se-Se structural fragments. There is no direct evidence from the present DSC, NMR, XPS, EXAFS and Raman investigations for the formation, in significant concentration, of over- and/or under-coordinated defects either on Se or As atoms, or for the existence of double-bonded Se or broken covalent bonds.

The proposed mechanisms of physical ageing are expected to be valid for As and/or Ge-based selenide glasses possessing underconstrained glass network with long or short Se chains between main structural units (pyramids or tetrahedra), respectively.

The author thanks U.S. National Science Foundation, through International Materials Institute for New Functionality in Glass (IMI-NFG), for initiating this international collaboration and providing partial financial support for this work (NSF Grant No. DMR-0409588). Special thanks to Dr. S Khalid of X18B NSLS for useful discussion and help in EXAFS measurements.

---

1. *Bureau B., Zhang X.H., Smektala F.* et al. Recent advances in chalcogenide glasses // J. Non-Cryst. Solids. 2004. Vol. 345&346. 276 p.
2. *Sanghera J.S., Aggarwal I.D.* Active and passive chalcogenide glass optical fibers for IR applications: a review // J. Non-Cryst. Solids. 1999. Vol. 256–257. 6 p.
3. *Churbanov M.F., Shiryaev V.S., Gerasimenko V.V.* et al. Stability of the optical and mechanical properties of chalcogenide fibers // Inorganic Materials. 2002. Vol. 38. 1063 p.
4. *Echeverria I., Kolek P.L., Plazek D.J., Simon S.L.* Enthalpy recovery, creep and creep–recovery measurements during physical aging of amorphous selenium // J. Non-Cryst. Solids. 2003. Vol. 324. 242 p.
5. *Drozdov A.D.* Physical aging in amorphous polymers far below the glass transition temperature // Computat. Mat. Sci. 1999. Vol. 15. 422 p.
6. *Struik L.C.E.* Physical ageing in amorphous polymers and other materials // Elsevier, New York. 1978.
7. *Golovchak R., Gorecki Cz., Kozdras A., Shpotyuk O.* Physical ageing effects in vitreous arsenic selenides // Sol. State Commun. 2006. Vol. 137. 67 p.
8. *Saiter J.M., Arnoult M., Grenet J.* Very long physical ageing in inorganic polymers exempli.ed by the Ge_xSe_{1-x} vitreous system // Physica B. 2005. Vol.355. 370 p.
9. *Golovchak R., Shpotyuk O., Kozdras A.* On the reversibility window in binary As-Se glasses // Phys. Let. A. 2007. Vol.370. 504 p.
10. *Stern E.A.* in: X-ray absorption: basic principles of EXAFS, SEXAFS and XANES // edited by D.C. Koningsberger & R. Prins. John Wiley & Sons, New York. 1988.

11. *Ravel B., Newville M.* ATHENA, ARTEMIS, HEPHAESTUS: data analysis for X-ray absorption spectroscopy using IFEFFIT // J. Synchrotron Rad. 2005. Vol. 12. 537 p.
12. *Renninger A.L., Averbach B.L.* Crystalline structures of As_2Se_3 and As_4Se_4 // Acta Cryst. B. 1973. Vol. 29. 1583 p.
13. *Kaplow R., Rowe T.A., Averbach B.L.* Atomic arrangement in vitreous selenium // Phys. Rev. 1968. Vol.168. 1068 p.
14. *Massiot D., Fayon F., Capron F.* et al. Modelling one- and two- dimensional solid state NMR spectra // Magnetic Resonance in Chemistry. 2002. Vol. 40. 70 p.
15. *Duddeck H.* Selenium-77 nuclear magnetic resonance spectroscopy // Progress in NMR spectroscopy. 1995. Vol. 27. 1 p.
16. *Moynihan C.T., Easteal A.J., Wilder J.* Dependence of the glass transition temperature on heating and cooling rate // J. Phys. Chem. 1974. Vol. 78. 2673 p.
17. *Nemilov S.V.* Physical ageing of silicate glasses at room temperature: general regularities as a basis for the theory and the possibility of a priori calculation of the ageing rate // Glass Phys. and Chem. 2000. Vol. 26. 511 p.
18. *Nemilov S.V.* Physical ageing of silicate glasses at room temperature: the choice of quantitative characteristics of the process and the ranking of glasses by their tendency to ageing // Glass Phys. and Chem. 2001. Vol. 27. 214 p.
19. *Galperin Yu.M., Karpov V.G., Kozub V.I.* Localized states in glasses // Adv. in Physics. 1989. Vol. 38. 669 p.
20. *Misawa M., Suzuki K.* // J. Phys. Soc. Japan. 1978. Vol. 44. 16125 p.
21. *Tichy L., Ticha H., Nagels P., Mertens R.* Photo-induced shifts in the optical gap of a-Se thin films // J. Optoel. Adv. Materials. 2002. Vol. 4. 785 p.
22. *Nakamura K., Ikawa A.* Medium range order in amorphous selenium: Molecular dynamics simulations // Phys. Rev. B. 2003.Vol. 67. 104203 p.
23. *Chakravarty S., Georgiev D. G., Boolchand P., Micoulaut M.* Ageing, fragility and the reversibility window in bulk alloy glasses // J. Phys.: Condens. Matter. 2005. Vol. 17. L1 p.
24. *Elssner G., Hoven H., Kiessler G., Wellner P.* Ceramics and ceramic composites: materialographic preparation. Elsevier. 1999.
25. *Bureau B., Troles J., Le Floch M., Smektala F.* et al. Solid state ^{77}Se NMR investigations on arsenic-selenium glasses and crystals // Solid State Sci. 2003. Vol. 5. 219 p.
26. *Georgiev D. G., Boolchand P., Micoulaut M.* Rigidity transitions and molecular structure of As_xSe_{1-x} glasses // Phys. Rev. B. 2000. Vol. 62. R9228 p.
27. *Nemilov S.V., Johari G.P.* A mechanism for spontaneous relaxation of glass at room temperature // Phil. Mag. 2003. Vol. 83. 3117 p.
28. *Varshneya A.K.* Fundamentals of inorganic glasses // Society of Glass Technology, 2006.
29. *Pauling L.* The nature of the chemical bond, 3rd ed. // Oxford and IBH New Dehli, 1967.
30. *Thorpe M.F., Jacobs D.J., Chubynsky M.V., Phillips J.C.* Self-organization in network glasses // J. Non-Cryst. Sol. 2000. Vol. 266–269. 859 p.
31. *Hatch C.T., Cerqua-Richardson K., Varner J.R., LaCourse W.C.* Density and microhardness of As-Se glasses and glass fibers // J. Non-Cryst. Solids. 1997. Vol. 209. 159 p.

32. *Nakamura K., Ikawa A.* Vibrational properties of a regular helical Se chain // Phys. Rev. B. 2002. Vol. 66. 024306 p.
33. *Bogomolov V.N., Poborchy V.V., Romanov S.G.* et al. Raman spectra of chalcogen chains isolated in zeolite matrixes // J. Phys. C: Solid State Phys. 1985. Vol. 18. L313 p.
34. *Kovanda V., Vlcek M., Jain H.* Structure of As–Se and As–P–Se glasses studied by Raman spectroscopy // J. Non-Cryst. Solids. 2003. Vol. 326&327. 88 p.
35. *Yannopoulos S.N., Andrikopoulos K.S.* Raman scattering study on structural and dynamical features of noncrystalline selenium // J. Chem. Phys. 2004. Vol. 121. 4747 p.
36. *Pauling L.* The nature of the chemical bond //Cornell Univ. Press, Ithaca. 1960.
37. *Golovchak R., Kovalskiy A., Miller A.C.* et al. The structure of Se-rich As-Se glasses by high-resolution X-ray photoelectron spectroscopy // Phys. Rev. B. 2007. Vol. 76. 125208 p.
38. *Kolobov A.V., Oyanagi H., Tanaka K., Tanaka Ke.* Photostructural changes in amorphous selenium: an in situ EXAFS study at low temperature // J. Non-Cryst. Solids. 1996. Vol. 198–200. 709 p.
39. *Chen G., Jain H., Khalid S., Li J.* et al. Study of structural changes in amorphous As_2Se_3 by EXAFS under in situ laser irradiation // Sol. State Commun. 2001. Vol. 120. 149 p.
40. *Minaev V.S., Timoshenkov S.P., Kalugin V.V.* Structural and phase transformations in condensed selenium // J. Optoel. Adv. Materials. 2005. Vol. 7. 1717 p.
41. *Renninger A. L., Averbach B.L.* Atomic radial distribution functions of As-Se glasses // Phys. Rev. B. 1973. Vol. 8. 1507 p.
42. *Newville M.* EXAFS analysis using FEFFand FEFFIT // J. Synchrotron Rad. 2001. Vol. 8. 96 p.
43. *Mauro J.C., Varshneya A.K.* Monte Carlo simulation of Se_xTe_{1-x} glass structure with ab initio potentials // Phys. Rev. B. 2005. Vol. 72. 024212 p.

СТРУКТУРНА МОДЕЛЬ КОРОТКО- І ДОВГОТЕРМІНОВОГО ФІЗИЧНОГО СТАРІННЯ В СЕЛЕН-ЗБАГАЧЕНИХ СТЕКЛАХ

Р. Головчак

Львівський науково-дослідний інститут матеріалів НВП "Карат"
вул. Стрийська 202, 79031 Львів, Україна

Довго- та короткотермінові компоненти ефекту фізичного старіння досліджено в Se-збагачених стеклах. На прикладі склоподібних $As_{10}Se_{90}$ та $As_{30}Se_{70}$ розглянуто особливості старіння As-Se стекол з довгими Se_n ланцюгами ($n \geq 3$) та стекол, структура яких наближається до самоорганізованої фази (оптимально-конструйованої сітки). Процеси, що відбуваються в разі фізичного старіння, досліджено методами диференціальної сканувальної калориметрії (DSC), рентгенівської фотоелектронної спектроскопії (XPS), ренгеноструктурної спектроскопії (EXAFS), ядерного магнітного резонансу на ^{77}Se (NMR) та спектроскопії комбінаційного розсіювання. На основі цих результатів запропоновано атомістичну модель фізичного старіння в As-Se стеклах.

Випрямлення-ущільнення полімерних Se ланцюгів визначено як основний мікроструктурний механізм короткотермінового фізичного старіння в Se-збагачених сіткових стеклах. Довготермінову ж компоненту фізичного старіння в стеклах з недокоординованою матрицею, яка характеризується короткими ланцюгами атомів селену ($1 \le n < 3$), пов'язано з кооперативною релаксацією багатьох атомів, сповільненою жорсткістю коротких полімерних ланцюгів Se за температур нижче температури розм'якшення скла.

Ключові слова: фізичне старіння, халькогенідне скло, EXAFS, NMR, DSC, спектроскопія комбінаційного розсіювання.

СТРУКТУРНАЯ МОДЕЛЬ КОРОТКО- И ДОЛГОСРОЧНОГО ФИЗИЧЕСКОГО СТАРЕНИЯ В СЕЛЕН-ОБОГАЩЕННЫХ СТЕКЛАХ

Р. Головчак

Львовский научно-исследовательский институт материалов НВП "Карат"
ул. Стрыйская 202, 79031 Львов, Украина

Долго- и краткосрочные компоненты эффекта физического старения исследовано в Se-обогащенных стеклах. На примере стекловидных $As_{10}Se_{90}$ и $As_{30}Se_{70}$ рассмотрены особенности старения As-Se стекол с длинными Se_n цепями ($n \ge 3$) и стекол, структура которых приближается к самоорганизованной фазе (оптимально-конструируемой сетки). Процессы, которые происходят в случае физического старения, исследовано методами дифференциальной сканированной калориметрии (DSC), рентгеновской фотоэлектронной спектроскопии (XPS), рентгеноструктурной спектроскопии (EXAFS), ядерного магнитного резонанса на ^{77}Se (NMR) и спектроскопии комбинационного рассеивания. На основе этих результатов предложена атомистическая модель физического старения в As-Se стеклах. Выпрямление-уплотнение полимерных Se цепей определено как основной микроструктурный механизм краткосрочного физического старения в Se-обогащенных сеточных стеклах. Долгосрочная же компонента физического старения в стеклах с недокоординированной матрицей, которая характеризируется короткими цепями атомов селена ($1 \le n < 3$), связана с кооперативной релаксацией многих атомов, замедленной жесткостью коротких полимерных цепей Se при температурах ниже температуры размягчения стекла.

Ключевые слова: физическое старение, халькогенидное стекло, EXAFS, NMR, DSC, спектроскопия комбинационного рассеивания.

Стаття надійшла до редколегії 04.06.2008
Прийнята до друку 25.03.2009